Available online at www.sciencedirect.com
ScienceDirect
Minerals Engineering 20 (2007) 1075–1088
MINERALS ENGINEERING
This article is also available online at: www.elsevier.com/locate/mineng

Chloride assisted leaching of chalcocite by oxygenated sulphuric acid via Cu(II)–OH–Cl

Gamini Senanayake *

Department of Mineral Science and Extractive Metallurgy, Murdoch University, Perth, WA 6150, Australia

Received 15 February 2006; accepted 17 April 2007
Available online 19 June 2007

Abstract

The beneficial effect of the addition of sodium chloride upon the leaching kinetics of complex iron–nickel–copper sulphides at elevated temperatures and oxygen pressures has been widely reported since the late 1970s, but the role of chloride is still being investigated or debated. Previous researchers have considered chloride as: (i) a complexing agent for cuprous ions; (ii) a surfactant that disperses the molten sulphur and thus removes passivation of the mineral surface by elemental sulphur during pressure leaching; and (iii) a reagent which increases the surface area and the porosity of the insoluble product layer on the surface. A proper understanding of the role of chloride based on the leaching of individual sulphides of known composition in the absence of host minerals at low pulp densities would be useful for the development of chloride assisted sulphate leaching processes for complex sulphide ores, concentrates, and mattes. In the present study evidence for the formation of basic salts of Cu(II) and Fe(III) during leaching are presented. The published rate data are analysed for the leaching of copper from mono-sized chalcocite particles in oxygenated sulphuric acid solutions maintained at 85 °C, a temperature lower than the melting point of sulphur. The initial leaching follows a shrinking particle (sphere) model, and the apparent rate constants are first order with respect to the concentration of dissolved oxygen and chloride. The intrinsic rate constant for the surface reaction (0.2 m s^{-1}) is two orders of magnitude larger than the calculated mass transfer coefficient of oxygen (3×10^{-3} m s^{-1}). The proposed reaction mechanism considers the formation of an interim $Cu(II)(OH)Cl^0$ species which facilitates the leaching process.

Keywords: Hydrometallurgy; Copper sulphide ores; Leaching; Kinetics

1. Introduction

The beneficial effect of chloride (0.5–10 g dm^{-3}), added as sodium chloride, to the leaching of iron–nickel–copper sulphide concentrates at 110 °C under an oxygen overpressure of 1.05 MPa has been reported by Subramanian and Ferrajuolo (1976). Recent publications have also identified that the addition of chloride at low concentrations has a significant beneficial effect on the kinetics of pressure leaching of sulphide ores/concentrates in oxygenated sulphuric acid media (Berezowsky and Trytten, 2002; Ferron et al., 2003; McDonald and Muir, 2007) and atmospheric leaching of chalcopyrite in ferric sulphate media (Carneiro and Leao, in press). For example, in the high pressure copper(II) leaching of copper–nickel sulphide and chalcopyrite with oxygen at high temperature (>130 °C) in sulphate media, the presence of low chloride (5–20 g dm^{-3}) improves the kinetics of leaching and achieves >95% metal extraction in relatively short retention times of 60–90 min (Subramanian and Ferrajuolo, 1976; Berezowsky and Trytten, 2002). In the case of atmospheric leaching of chalcopyrite in oxygenated ferric sulphate solutions at 95 °C the copper extraction after 10 h was 91% in the presence of 1 mol dm^{-3} sodium chloride, compared to 45% in the absence of chloride (Carneiro and Leao, in press).

Dreisinger (2006) reviewed the various process options for copper leaching from primary sulphides and described the chemical reactions, advantages, and disadvantages of

* Tel.: +61 8 93602833; fax: +61 8 93606343.
E-mail address: g.senanayake@murdoch.edu.au

0892-6875/$ - see front matter © 2007 Elsevier Ltd. All rights reserved.
doi:10.1016/j.mineng.2007.04.002

selected process options. Fine grinding combined with low chloride addition has been responsible for the success of the ACTIVOX (Johnson and Streltsova, 1999) and PLASTOL (Ferron et al., 2003) processes. Peacey et al. (2003) reviewed the chloride assisted sulphate processes which made use of oxygenated solutions at atmospheric (BHAS) or elevated (Noranda, CESL) pressures. Defreyne et al. (2006) described the CESL pressure oxidation of base metal concentrates at elevated temperatures in mixed sulphate–chloride liquor at pH 2–3 to achieve maximum oxidation of metals with minimum oxidation of sulphide to sulphate, leading to low oxygen consumption. In the case of chalcopyrite concentrates it produces basic copper sulphate precipitate at pH 2–3 which requires a subsequent atmospheric-acid leach, but minimises the dissolution of iron. The practical advantages of chloride also include higher crystalanity of sulphur and insignificant oxidation of sulphide to sulphate (Muir and Ho, 1996). The chloride addition has a more important role on leaching chalcopyrite with oxygenated ferric sulphate than with ferric chloride (Carneiro and Leao, in press). However, in many examples reported in the literature, an increase in background chloride beyond a certain level up to 0.5–1 mol dm^{-3} in sulphate systems does not show a significant influence on the leaching kinetics and the final metal extraction (Cheng and Lawson, 1991a,b; Lu et al., 2000a,b; Deng et al., 2001; Ferron et al., 2002; Carneiro and Leao, in press).

The analysis and rationalisation of the effect of chloride on kinetics of copper–iron–nickel mixed sulphide concentrates or mattes is complicated due to a number of reasons. Firstly, the ore/concentrate often contains a number of different sulphides such as chalcopyrite, pyrite, pyrrhotite, chalcocite, covellite, and pentlandite in which some host minerals can affect the leaching kinetics of a given sulphide due to galvanic effects (Provis et al., 2003). Secondly, it is also possible that cations such as copper(II) and iron(III) dissolved from host minerals catalyse the oxidation reaction by oxygen. For example, Parker et al. (1981) showed that a mixture of Fe(III)/Cu(II)/Cl^- is one of the more effective oxidants of chalcopyrite due to the faster reduction of copper(II) to copper(I) compared with iron(III) to iron(II), on a corroding chalcopyrite surface. Copper(I) is oxidized to copper(II) by iron(III) or oxygen to continue the redox cycle as shown in the E_H–log[Cl^-] diagram in Fig. 1a. Thirdly, the rates will also depend on the actual concentration of dissolved oxygen which in turn is dependent on the salt or acid content in solution, partial pressure, and temperature. In the case of sulphuric acid solutions, the sulphate/bisulphate equilibrium and temperature govern the actual concentration of H^+. Fourthly, the state of elemental sulphur also affects the leaching kinetics. Pressure oxidation of sulphides are more favourable at temperatures above the melting point of sulphur (119 °C). Recent studies (Dreisinger et al., 2003; Brown and Papangelakis, 2005) have shown that while the molten elemental sulphur occluded on unreacted mineral surface inhibits the

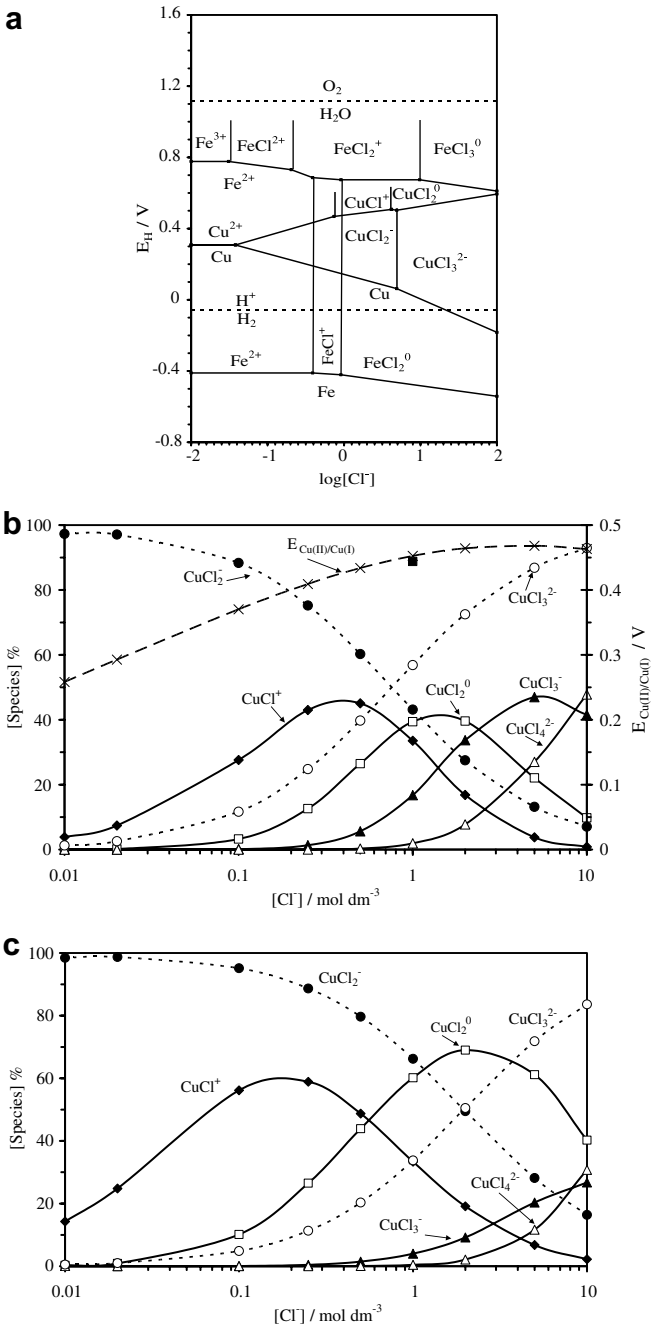

Fig. 1. E_H–log[Cl^-] and species distribution diagram for iron–copper–chloride–water system: (a) at 25 °C and 100 mol dm^{-3} metal ions; (b) at 25 °C, 1 mol m^{-3} Cu(II)/(I), measured platinum electrode E_H in 0.5 mol dm^{-3} $CaCl_2$ shown by ■; (c) at 100 °C, 1 mol m^{-3}Cu(II)/(I).

diffusion of dissolved oxygen and retards the reaction, both chloride ions and sulphur dispersing surfactants such as ligninsulphonate lower the interfacial tension between liquid sulphur and the aqueous solution. The dispersion of molten sulphur by a surfactant avoids the passivation during leaching.

Rate analysis of solid dissolution generally considers either a chemical reaction at the surface, or diffusion or mass transfer of reactants or products. The results from such studies are quantified on the basis of a first order

heterogeneous rate constant ($k_{apparent}$, s^{-1}), a diffusion coefficient (D, $m^2\,s^{-1}$), or an external mass transfer coefficient (k_m, $m\,s^{-1}$), respectively, where k_m is the ratio D/δ, and δ is the diffusion layer (film) thickness (Cussler, 1997). A non-porous shrinking particle (sphere) kinetic model (Levenspiel, 1972) described by Eq. (1) considers: (i) a first order surface reaction, $A(aq) + bB(s) \rightarrow$ products, of a solid B with a reactant A of concentration C ($mol\,m^{-3}$) in solution, and (ii) a decrease in surface area due to the decrease in initial particle radius r_0 (m) with time t (s). The terms ρ ($mol\,m^{-3}$) and k_{ss} (s^{-1}) represent the molar concentration of reacting metal in solid B and the apparent rate constant respectively, while X represents the fraction of metal leached after time t. The intrinsic rate constant k has the same units as the mass transfer coefficient k_m.

$$1-(1-X)^{1/3}=\left(\frac{bkC}{r_0\rho}\right)t=k_{ss}t \tag{1}$$

This model has been used to examine whether the dissolution of gold colloids (McCarthy et al., 1998), and oxides such as manganese dioxide (Miller and Wan, 1983) and magnesium oxide (Raschman and Fedorockova, 2006) occur under mass-transfer control conditions. In all cases, the comparison between rate constant (k) and the mass transfer coefficient (k_m) showed that the overall rate of dissolution is controlled by the rate of surface reaction rather than the rate of mass transfer of reagents to the surface. Similar studies will shed more light on surface reactions, mechanisms and the role of chloride ion in chloride assisted leaching of sulphides, which in turn will lead to further studies on developing leaching processes for complex-sulphides concentrates and mattes.

While the results from electrochemical and chemical leaching tests suggest that the formation of elemental sulphur, chalcocite, covellite (or copper rich polysulphides), and precipitation of iron-hydroxy compounds are responsible for the slow kinetics during the leaching of chalcopyrite (Okamoto et al., 2003; Tshilombo and Dixon, 2003), the copper sulphides also play an important role in the leaching of nickel from mattes (Muir and Ho, 1996; Rademan et al., 1999; Provis et al., 2003). Peters (1976) described a non-oxidative pathway for the dissolution of chalcopyrite according to Eq. (2). Nicol and Lazaro (2003) described the role of the non-oxidative dissolution process and proposed the dissolution of chalcopyrite according to Eq. (2) at a maximum rate given by Eq. (3):

$$CuFeS_2 + 4H^+ = Cu^{2+} + Fe^{2+} + 2H_2S \tag{2}$$

$$\text{Maximum rate} = k_m(4K)^{1/4}[H^+] \tag{3}$$

where, K is the equilibrium constant for Eq. (2) ($K = 6.53\times10^{-18}$ at 60 °C) and k_m is the external mass transfer coefficient ($k_m = 1.8\times10^{-5}\,m\,s^{-1}$ equivalent to a rotating disc at 200 rpm). Thus, they calculated a maximum rate of dissolution of copper ($6.5\times10^{-8}\,mol\,m^{-2}\,s^{-1}$) at $[H^+] = 0.1\,mol\,dm^{-3}$, a value which was remarkably similar to an experimental value of $5.3\times10^{-8}\,mol\,m^{-2}\,s^{-1}$ at 60 °C. Miki et al. (2003) proposed that catalysts such as silver(I), bismuth(III), and activated carbon remove the hydrogen sulphide formed during chalcopyrite reduction to chalcocite, causing a rapid copper extraction due to oxidative dissolution of the intermediate chalcocite by iron(III). These findings also highlight the importance of extending the rate analysis of the dissolution of sulphide minerals at a fundamental level in order to rationalise the kinetics of individual sulphides such as chalcocite and covellite of known composition (synthetic sulphides) in the absence of impurities at a low pulp density.

Previous researchers have carried out detailed studies of the effect of oxygen flow rate, agitation, and acid or chloride concentration on copper extraction from synthetic chalcocite and covellite (Cheng and Lawson, 1991a,b; Vracar et al., 2000), digenite concentrate (Ruiz et al., 1998), and copper residues produced by selective oxidative leaching of a nickel matte (Deng et al., 2001). Lu et al. (2000a,b) extended the kinetic studies to chalcopyrite and pentlandite. The aims of previous studies were to quantify the effect of experimental variables and to rationalise the role of chloride. For example, Cheng and Lawson (1991a) reviewed the previous studies and conducted experiments to show that at a low pulp density of 1 g dm^{-3} the increase in temperature (65–94 °C), partial pressure of oxygen (5–100%), concentration of chloride (0–2 mol dm^{-3} NaCl), and the decrease in particle size (58–12 μm) enhanced the initial rate of leaching of synthetic chalcocite. The increase in acid concentration (0.02–2.0 mol dm^{-3} H_2SO_4), agitation, and the nature of acid (HCl, HNO_3 or H_2SO_4) had no significant influence on leaching kinetics in the presence of chloride. Although the formation of basic copper chlorides of the form $Cu(OH)Cl_x^{(1-x)}$ and $Cu_2(OH)_3Cl$ have been reported (McDonald and Langer, 1983; Cheng and Lawson, 1991b; Muir, 2002), no attempt has been made to incorporate basic salts in the reaction mechanism to rationalise the leaching kinetics.

Considering the importance of chalcocite as a component of secondary enriched copper deposits, copper/nickel mattes, and white metal (Rademan et al., 1999; Provis et al., 2003; Ruiz et al., 2007), and the relative simplicity of its initial dissolution, this paper aims to investigate and discuss the role of chloride ions in chalcocite leaching under the following topics:

(i) review the current status of relevant chemical speciation in solution, and reaction mechanism of initial chalcocite leaching by oxygenated sulphuric acid;
(ii) quantify the effect of particle size, sulphuric acid, oxygen, and chloride concentration on the basis of a shrinking sphere kinetic model and examine whether the initial leaching reaction of chalcocite occurs under mass transfer controlled conditions; and
(iii) propose a kinetic model for the initial surface chemical reaction based on surface adsorption of reactants and the formation of $Cu(OH)Cl^0$ as an interim copper(II) species.

2. Chemical speciation

2.1. Copper speciation in chloride solutions

It is clear that Cu^{2+}, $CuCl^{+}$ and $CuCl_2^{-}$ are the stable copper(II)/(I) species at 25 °C in solutions of chloride concentrations in the range 0.02–2 mol dm^{-3} (Fig. 1a) (Senanayake and Muir, 2003). However, it is important to consider the effect of temperature on speciation since Cheng and Lawson (1991a) conducted experiments at higher temperatures (65–94 °C). McDonald et al. (1987) predicted the change in equilibrium constants for copper(I) and copper(II) in chloride solutions with the increase in temperature from 25 to 102 °C using the Van't Hoff equation $(\mathrm{d}\ln K/\mathrm{d}T)_p = \Delta H^\circ/RT^2$. Fig. 1b–c compare the effect of chloride concentration on species distribution at 25 and 102 °C, respectively, based on equilibrium constants listed in Table 1. Fig. 1b shows that $CuCl^{+}$ is the predominant copper(II) species at low chloride concentrations (<0.5 mol dm^{-3}), while $CuCl_2^{-}$ is the predominant copper(I) species (<0.8 mol dm^{-3}) at 25 °C. The reduction potential of the copper(II)/copper(I) couple based on $E_{Cu(II)/Cu(I)} = 0.15 + 0.059\log\{[Cu^{2+}]/[Cu^{+}]\}$ V at 25 °C is also plotted in Fig. 1b. The measured value of $E_{Cu(II)/Cu(I)} \approx 0.45$ V (Senanayake and Muir, 1988) and the predicted value in this work (Fig. 1b) in a solution of 1 mol dm^{-3} chloride ions is in reasonable agreement with the value of E_H shown in Fig. 1a. As shown in Fig. 1c, the copper(II) species $CuCl_2^0$ is more stable at higher temperatures (102 °C) and higher chloride concentrations. However, $CuCl^{+}$ is the predominant species at low chloride concentrations (<0.5 mol dm^{-3}) while $CuCl_2^{-}$ remains predominant at chloride concentrations <1 mol dm^{-3} at 102 °C.

2.2. Copper speciation in mixed chloride–sulphate solutions

The dissociation of sulphuric acid can be represented by Eqs. (4) and (5).

$$H_2SO_4 \rightarrow H^+ + HSO_4^- \quad (4)$$

$$HSO_4^- = H^+ + SO_4^{2-} \quad (5)$$

Table 1
Equilibrium constants (K)

Equilibrium	K at 25 °C	K at 85 °C	K at 102 °C
$Cu^+ + 2Cl^- = CuCl_2^-$	6.9×10^5	–	9.6×10^5
$Cu^+ + 3Cl^- = CuCl_3^{2-}$	9.1×10^5	–	4.9×10^5
$Cu^{2+} + Cl^- = CuCl^+$	4.0	–	17
$Cu^{2+} + 2Cl^- = CuCl_2^0$	4.7	–	30
$Cu^{2+} + 3Cl^- = CuCl_3^-$	2.0	–	2.0
$Cu^{2+} + 4Cl^- = CuCl_4^{2-}$	0.23	–	0.23
$Cu^{2+} + SO_4^{2-} = CuSO_4^0$	2.1×10^2	–	8.3×10^2
$Na^+ + SO_4^{2-} = NaSO_4^-$	5.2	11	13
$H^+ + SO_4^{2-} = HSO_4^-$	98	6.5×10^2	1.2×10^3
$Cu^{2+} + HSO_4^- = CuSO_4^0 + H^+$	2.0	–	0.69
$Na^+ + HSO_4^- = NaSO_4^- + H^+$	0.05	0.02	0.01

Copper(II) chloride data from McDonald et al. (1987); copper(II) sulphate data from Mendez De Leo et al. (2005); sodium sulphate data from Hogfeldt (1982).

The first dissociation described by Eq. (4) goes to completion. The equilibrium constant (K_a) for the second dissociation (Eq. (5)) changes with temperature. The reported values of K_a (Hogfeldt, 1982) fit the equation:

$$\log K_a = 0.0143T - 2.3074 \ (R^2 > 0.99) \quad (6)$$

which gives a value of $\log K_a = 2.81$ at 85 °C. This value was used to calculate the concentration of H^+, HSO_4^- and SO_4^{2-} shown in Fig. 2a. Thus, the concentration of sulphate ions formed in the second dissociation given by Eq. (5) is negligibly small and can be ignored in the present study.

However, in the presence of sodium chloride, the association between sodium and sulphate ions (Table 1) can affect the sulphate/bisulphate equilibrium. Thus, Fig. 2b shows that in the presence of sodium ions the concentration of H^+ is larger than that of HSO_4^-. In a mixed chloride–sulphate system it is important to consider the effect of the association between copper(II) and sulphate ions as revealed by the equilibrium constants listed in Table 1. Thus, as shown in Fig. 2c, $Cu(SO_4)^0$ is the most predominant species (73–100%) in solutions of 0.5 mol dm^{-3} H_2SO_4 + NaCl. At a very low chloride concentration (0.01 mol dm^{-3}) Cu^{2+} ions (24%) are more predominant than $CuCl^{+}$ (4%). However, $CuCl^{+}$ concentration exceeds that of Cu^{2+}at [Cl^-] >0.05 mol dm^{-3}. This highlights the importance of considering the formation of such species in solution or sold phase which would be converted to a more stable sulphate species $Cu(SO_4)^0$ in solution.

2.3. Formation of basic salts during non-chloride leaching

In a comprehensive modelling study of chalcocite column and heap bioleaching in a non-chloride system, Dixon and Petersen (2003) noted the formation of $Cu_{1.2}S$, and $CuSO_4 \cdot 3Cu(OH)_2$ while the rate of copper recovery was controlled primarily by those factors which influence the kinetics of covellite oxidation. Grewal et al. (1992) studied the leaching of Cu_2S-containing residue (55–60% Cu, 6–10% Ni, 6–10% Co, 4–9% Fe, 13–19% S) to investigate the different stages of leaching in a non-chloride system. The leaching was conducted in a pressure autoclave at 1.034 MPa and 115 °C (820 rpm) using a synthetic spent electrowinning electrolyte. The leaching by 40 g dm^{-3} Cu (as $CuSO_4$), 5 g dm^{-3} Fe (as $FeSO_4$) and 200 g dm^{-3} sulphuric acid at a high pulp density (0.51 kg feed/0.5 dm^3 electrolyte) produced covellite and basic copper(II) sulphate (Eqs. (7) and (8)).

$$Cu_2S + H_2SO_4 + 0.5O_2 = CuS + CuSO_4 + H_2O \quad (7)$$

$$Cu_2S + 0.5CuSO_4 + 0.5O_2 + H_2O = CuS + 0.5(2Cu(OH)_2 \cdot CuSO_4) \quad (8)$$

$$CuS + 2O_2 = CuSO_4 \quad (9)$$

$$CuS + H_2SO_4 + 0.5O_2 = CuSO_4 + H_2O + S^0 \quad (10)$$

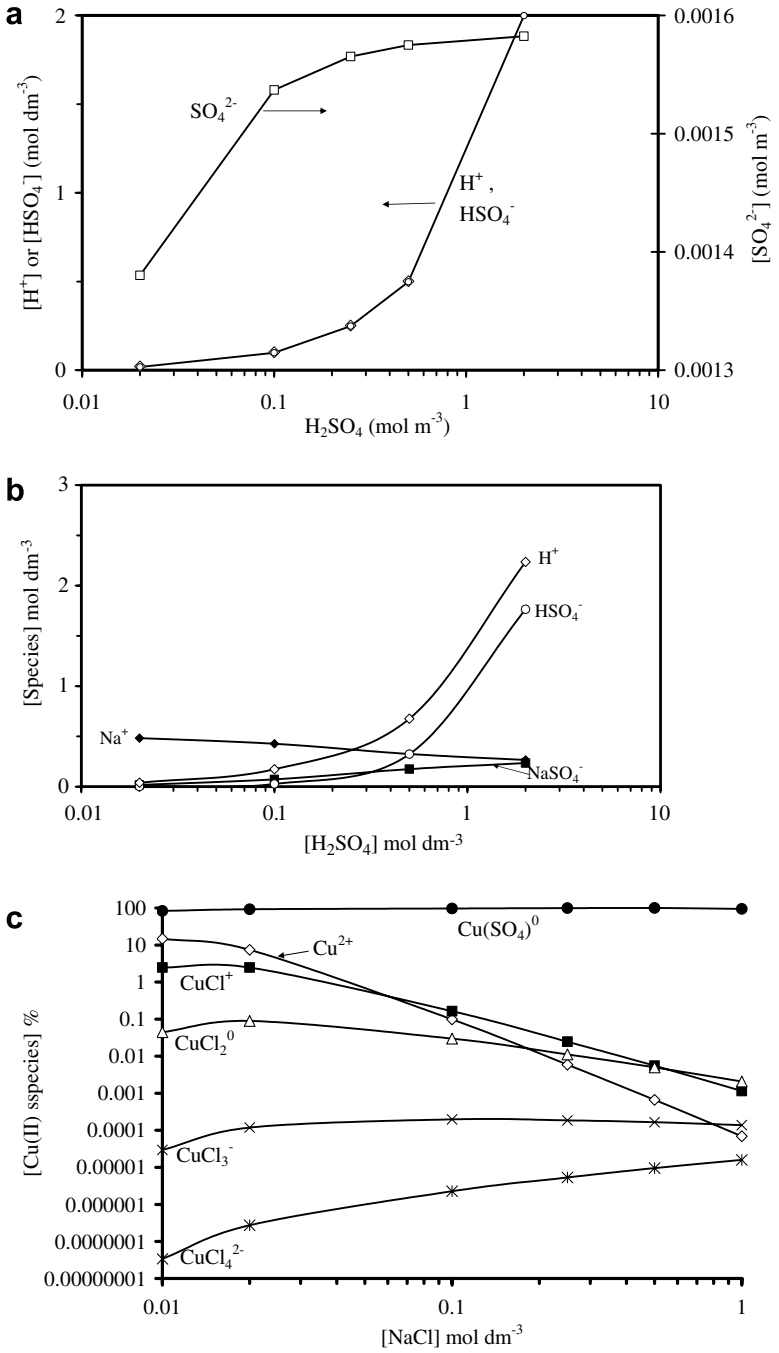

Fig. 2. Effect of sulphuric acid and sodium chloride on speciation: (a) H_2SO_4 in the absence of chloride, 85 °C; (b) H_2SO_4 in the presence of 0.5 mol dm^{-3} NaCl, 85 °C; (c) 1 mol m^{-3} Cu(II) + 0.5 mol dm^{-3} H_2SO_4, 102 °C (see text).

The X-ray diffraction results showed the formation of Cu_xS intermediates, where the value of x changed from 2 to 0 as the oxygen consumption increased from 0% to 48%. The rates of leaching of the observed intermediates ($Cu_{1.96}S$, $Cu_{1.76}S$, etc.) were faster than that of CuS. Although the reactions given by Eqs. (7)–(10) take place concurrently, the leaching of CuS according to Eq. (9) was observed only in low pulp density leaches. A deficiency of iron in solution increased the viscosity of the product slurry, which in turn decreased oxygen mass transfer leading to slow kinetics and extended leaching time (Grewal et al., 1992).

2.4. Formation of basic salts during chloride-assisted leaching

The CESL copper process which uses a chloride assisted acid-leaching of chalcopyrite also produces a basic copper sulphate precipitate in the autoclave according to Eq. (11) (Defreyne et al., 2006). In this process, the chalcopyrite slurry is fed to the pressure autoclave and treated with oxygen and recycled process liquor containing approximately 12 g dm^{-3} chloride, 25 g dm^{-3} sulphate, and iron (<1.0 g dm^{-3}). In the atmospheric leach circuit, the filter

cake from pressure oxidation/thickening/filtration is repulped in the raffinate from the solvent extraction circuit at pH 1.4–1.8. This is used to leach the basic copper sulphate (Eq. (12)) to extract 96–98% copper with only 2.1 g dm^{-3} iron in the pregnant leach liquor (Defreyne et al., 2006).

$$3CuFeS_2 + 3.75O_2 + H_2O + H_2SO_4 = Cu(SO_4) \cdot 2Cu(OH)_2 + 1.5Fe_2O_3 + 6S^0 \quad (11)$$

$$Cu(SO_4) \cdot 2Cu(OH)_2 + 2H_2SO_4 = 3CuSO_4 + 4H_2O \quad (12)$$

The equilibrium constant for the conversion of hematite (α-Fe_2O_3) to goethite (α-FeOOH) according to Eq. (13) is 1.2 at 25 °C (Flynn, 1984). However, the published temperature-pH-speciation diagram for Fe^{3+} ions, its hydroxyl species, hematite, and goethite show that at temperatures above 100 °C and pH above 2.2 hematite is the most stable product (Claassen et al., 2003). Thus, under the typical conditions of pressure oxidation in the CESL process (150 °C, pH 3) iron produces hematite while the copper sulphide minerals are oxidized to basic copper(II) sulphate (Eq. (11)).

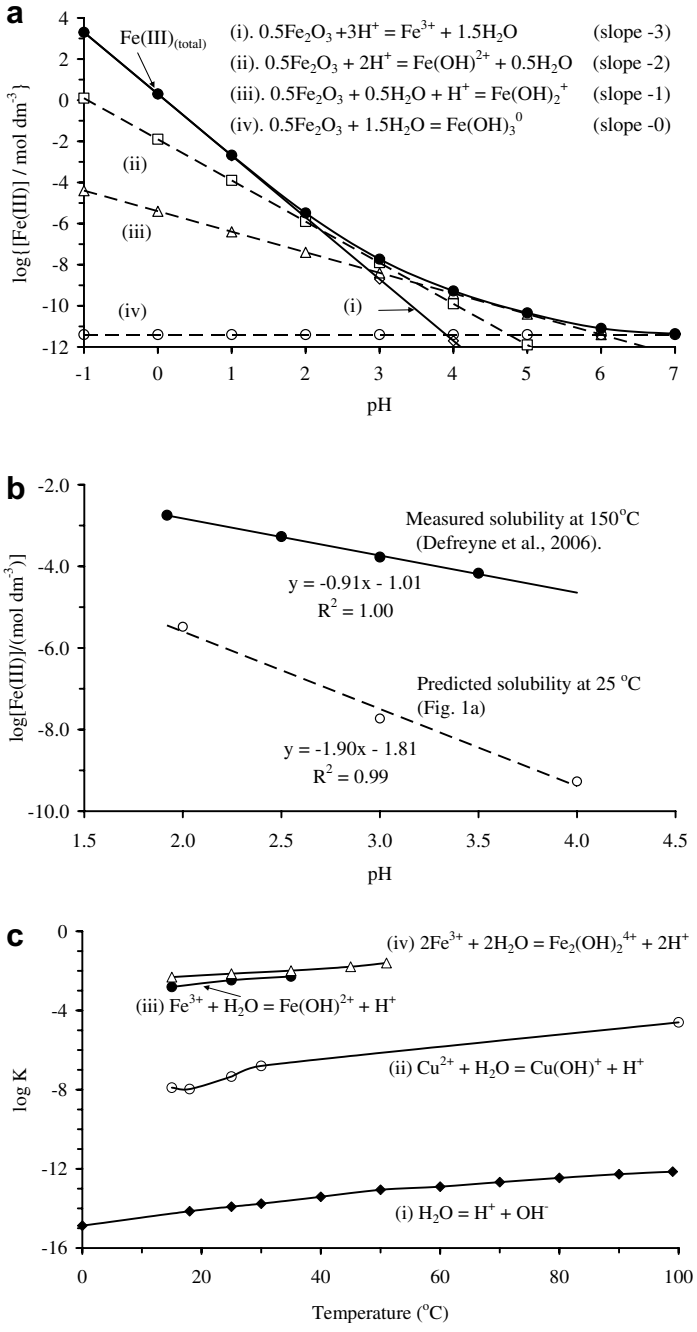

Fig. 3. Dependence of iron solubility on pH and equilibrium constant on temperature: (a) predicted [Fe(III)] in water at 25 °C; (b) measured [Fe(III)] in autoclave discharge in the chloride assisted oxygen-pressure leaching of copper in CESL process at 150 °C (Defreyne et al., 2006); (c) reported *K* values (Sillen and Martell, 1964; Hogfeldt, 1982).

$$0.5Fe_2O_3 + 0.5H_2O = FeOOH \quad (13)$$

$$FeOOH + H^+ + X^- = Fe(OH)_2X \quad (14)$$

$$0.5Fe_2O_3 + 0.5H_2O + H^+ + X^- = Fe(OH)_2X \quad (15)$$

Due to strongly oxidizing conditions in the pressure oxidation step the dissolved iron was in the form of iron(III), and remained at 10 mg dm^{-3} at steady state leaching in the CESL process. The iron content in the autoclave discharge decreased with increasing pH. Fig. 3a shows the predicted logarithmic solubility of iron from hematite at 25 °C as a function of pH, based on the thermodynamic data reported by Flynn (1984), to highlight the different slopes representing the solubility of iron in the form of different species: (i) Fe^{3+} (slope −3); (ii) $Fe(OH)^{2+}$ (slope −2); (iii) $Fe(OH)_2^+$ (slope −1); and (iv) $Fe(OH)_3$ (slope 0). The decrease in the predicted overall solubility of iron(III) is also shown in Fig. 3a.

The measured solubility of iron(III) in the autoclave discharge of the CESL process as a function of pH, shown in Fig. 1b, indicates higher iron solubility and a slope of 0.9. The slope close to unity is consistent with a di-hydroxy species of the type $Fe(III)(OH)_2X$ represented by Eq. (15) which is the sum of Eqs. (13) and (14). The higher solubility is consistent with the enhanced stability of $Fe(OH)_2^+$ at higher temperatures. For example, the hydrolysis constant (K_h) for the reaction $Fe^{3+} + 2H_2O = Fe(OH)_2^+ + 2H^+$ remains unchanged with an increase in ionic strength from 0 to 2.67, but increases with temperature at a given ionic strength of 2.67 from $K_h = 2 \times 10^{-6}$ (25 °C) to $K_h = 6 \times 10^{-4}$ (80 °C) (Flynn, 1984). The cationic nature of the iron(III) species is also evident from a ratio of $OH^-/Fe(III) = 2.25$ in the isolated hydrolytic polymers formed as amorphous solids due to mixing of ferric nitrate and chloride solutions (Flynn, 1984).

Carneiro and Leao (in press) reported interesting observations and conclusions in relation to chloride assisted copper leaching from chalcopyrite by oxygenated iron(III) sulphate at 95 °C. The measured potential in the range 0.700–0.425 ($Ag/AgCl/Cl^-$ electrode) translates to E_H in the range 0.900–0.625 V corresponding to the equilibria $Fe(III) + Cu(I) = Fe(II) + Cu(II)$ (Fig. 1a), but the first order rapid oxidation of copper(I) by oxygen (Hine and Yamakawa, 1970) and the higher stability of $Cu(SO_4)^0$ (Fig. 1c) would result low copper(I). In the presence of sodium chloride the iron(II) concentration was higher but the total iron(II)/(III) concentration was lower due to the precipitation of natrojarosite $Na[Fe(III)(OH)_2]_3(SO_4)_2$. While natrojarosite was not observed in the absence of sodium chloride the observed higher iron(III) concentration did not assist the leaching kinetics or final copper extraction. Moreover, the leaching kinetics of chalcopyrite leaching by oxygenated iron(III) sulphate in the absence of sodium chloride showed diffusion through reaction products on the surface. In the presence of sodium chloride the leaching kinetics changed to mixed (chemical reaction and diffusion) control suggesting a change in reaction mechanism due to chloride (Carneiro and Leao, in press).

The increase in the dissociation constant of water (line i) and the hydrolysis constants of Cu^{2+} (line ii) and Fe^{3+} (lines iii and iv) in Fig. 3c rationalises the formation of basic salts at elevated temperatures in Eqs. (8), (11) and (15). The formation of natrojarosite in atmospheric leaching of chalcopyrite in iron(III) sulphate media is also consistent with the formation of dihydroxy iron(III) species in the presence of chloride ions. Yet, the role of chloride ions in the surface reaction is not directly evident in reactions represented by Eqs. (7)–(12). However, the beneficial effect of chloride on the rate of dissolution of goethite and copper(II) oxide has been related to the formation of the interim species $Cu(OH)Cl^0$ and $Fe(OH)_2Cl^0$ (Senanayake, 2007b). Cheng and Lawson (1991b) identified a basic copper(II) chloride species $Cu(OH)Cl \cdot Cu(OH)_2$ formed during the chloride assisted leaching of covellite by oxygen at a low (5×10^{-3} mol dm^{-3}) initial sulphuric acid concentration. It is useful to: (i) review the current status of the reaction mechanism of the oxidation of chalcocite by oxygen and the role of chloride; and (ii) incorporate hydroxyl species of copper(II) such as $Cu(OH)Cl^0$ to rationalise the beneficial effect of chloride in the leaching of chalcocite.

3. Current status of reaction mechanism and the role of chloride

The leaching of chalcocite by oxygen is a two stage reaction (Sullivan, 1933; Cheng and Lawson, 1991a). The leaching reaction in both stages is electrochemical in nature as described by Eqs. (16) and (17), leading to the overall reactions in Eqs. (19) and (20). The two stage chloride assisted leaching of chalcocite has been confirmed in several studies by conducting batch leaching experiments with: (i) $Cu_2S/NaCl/H_2SO_4$ (Cheng and Lawson, 1991a); (ii) $Cu_{1.8}S/HCl/NaCl$ (Ruiz et al., 1998); and (iii) $Cu_2S/HCl/CaCl_2$ (Vracar et al., 2000) over the temperature range 75–150 °C.

$$Cu_2S = Cu^{2+} + CuS + 2e^- \quad (16)$$

$$CuS = Cu^{2+} + S + 2e^- \quad (17)$$

$$2H^+ + 0.5O_2 + 2e^- = H_2O \quad (18)$$

$$Cu_2S + 2H^+ + 0.5O_2 = Cu^{2+} + CuS + H_2O \quad (19)$$

$$CuS + 2H^+ + 0.5O_2 = Cu^{2+} + S + H_2O \quad (20)$$

In preliminary modelling Cheng and Lawson (1991a) considered that during the first stage cuprous ions diffuse from the interior of particles to the surface, whilst the dissolved oxygen diffuses through the liquid boundary layer to the particle surface and reacts with cuprous ions and causes the formation of copper-deficient Cu_xS intermediates. However, the fraction of copper diffused (as predicted) on the basis of $D_{Cu}^+ = 1.43 \times 10^{-9}$ cm^2 s^{-1} at 85 °C for copper diffusivity through the solid phase, was larger than the fraction dissolved (as measured). Moreover, if oxygen mass transfer is the rate controlling step, the oxygen concentration at the particle surface will be nearly zero due to the

faster surface reaction, and oxygen diffusion past the surface into the pores will not occur. Hence, both the diffusion of cuprous ions through the solid phase and oxygen through the pores to react with cuprous are unlikely to be the rate controlling steps (Cheng and Lawson, 1991a). Although previous reports have noted that the role of chloride is to stabilise cuprous as $CuCl_2^-$ ions, Cheng and Lawson (1991a) noted that $CuCl_2^-$ in solution is only stable in oxygen deficient solutions. They reported that only higher pulp densities may favour $CuCl_2^-$ because there is no adequate mass transfer of oxygen into the liquid phase.

As covellite is formed on the outer surface it begins to react, leaving a shell of sulphur surrounding the shrinking core of unreacted covellite (Cheng and Lawson, 1991a). Thus, the oxygen leaching of covellite (second stage, Eq. (20)) proceeds in parallel with the first stage (Eq. (19)) but at a much slower rate, and only becomes significant when about 40% of the initial copper has been leached. The coherent layer of sulphur on the particle surface protects the sulphide material from attack by leachant. The rate of the second stage increased after the removal of elemental sulphur (by washing the leach residue) showing that the surface passivation layer was not a metal-deficient sulphide, rather a layer of elemental sulphur (Cheng and Lawson, 1991a). The slow leaching of covellite compared to chalcopyrite and chalcocite is also evident from the experimental results based on iron(III) sulphate leaching at low temperatures listed in Table 2, as the acid–oxygen pressure leaching of chalcocite displays the same two-stage leaching characteristics as iron(III) sulphate leaching (Mao and Peters, 1983).

In the case of chalcocite leaching, the chloride ions disrupts the passivating sulphur layer and accelerate the first stage reaction, making the second stage reaction possible, because the growing well defined porous crystalline sulphur layer allows reactants to pass through it in the presence of chloride (Cheng and Lawson, 1991a). Moreover, due to the beneficial effect of chloride, the leaching curves of chalcocite over a period of 3 h in: (a) 0.5 mol dm^{-3} HCl, (b) 0.5 mol dm^{-3} HNO_3 + 0.5 mol dm^{-3} NaCl, and (c) 0.25 mol dm^{-3} H_2SO_4 + 0.5 mol dm^{-3} NaCl, were essentially the same with copper extraction of over 95% and <1% sulphur converted to sulphate in both (a) and (b).

The activation energy for the first and second stage of chloride assisted leaching of chalcocite was 33.5 and 69.0 kJ mol^{-1}, respectively (Cheng and Lawson, 1991a). However, in the absence of chloride ions these values increase to 55 and 88 kJ mol^{-1} respectively in sulphuric acid–oxygen pressure leaching (Ruiz et al., 2007), highlighting the involvement of chloride ions in the surface reaction in both stages. The anodic dissolution of synthetic chalcocite particles (+325 mesh) in a fluidised bed at a mixed sulphuric acid–sodium chloride electrolyte flow (0.4 dm^3 min^{-1}) and temperatures of 40 or 90 °C also showed a two stage leaching of chalcocite (MacKinnon, 1976). The first stage involved the formation of $Cu_{1.1}S$ (Eq. (21)), while the second stage was attributed to the reaction between chloride and $Cu_{1.1}S$ with an overall copper extraction of 95% in 14–16 h. The increase in sodium chloride content in the electrolyte from 25 to 50 kg m^{-3} increased the rate of both stages of dissolution by a similar amount. Again, the role of sodium chloride in the anodic reaction remains unclear. These findings highlight the importance of a systematic analysis of rate data for chalcocite to examine the reaction order with respect to each reagent.

$$Cu_2S(s) = Cu_{1.1}S(s) + 0.9Cu^{2+} + 1.8e^- \quad (21)$$

4. Initial rates: effect of reagent concentration

Table 3 lists the general conditions used by Cheng and Lawson (1991a) and some of the variables which are used in the present analysis: oxygen % in the bubbling gas (A1–A6), sodium chloride concentration (B1–B5), and sulphuric acid concentration (C1–C4). Fig. 4a shows a plot of X as a function of time to highlight the effect of increasing oxygen % in bubbling gas on the fraction of copper leached. The variation of X versus time is linear for results obtained using low oxygen % (A1–A3). Fig. 4b shows a plot of $1-(1-X)^{1/3}$ as a function of t for the results reported by Cheng and Lawson (1991a) for the initial

Table 2
Relative extraction of copper by acidic $Fe_2(SO_4)_3$

Mineral	35 °C		50 °C	
	Time/days	%Cu	Time/days	%Cu
Bornite	–	–	3	85
Chalcocite	1	50	8	95
Chalcopyrite	–	–	14	44
Covellite	11	35	50	70
Enargite	–	–	60	5

Mesh size −100 + 200, (Taylor, 1995; Peacey et al., 2003).

Table 3
Test conditions used by Cheng and Lawson (1991a)

Test	Size (μm)	$[H_2SO_4]$ (mol dm^{-3})	NaCl (M) (mol dm^{-3})	$[O_2]$ (%)	$10^5 k_{ss}$ (s^{-1})
A1	23	0.5	0.5	5	2.50
A2				21	9.50
A3				39	18.7
A4				59	31.8
A5				81	30.7
A6				100	42.7
B1	31	0.5	0.02	100	3.67
B2			0.10		16.2
B3			0.25		32.3
B4			0.50		36.5
B5			2.0		39.0
C1	31	0.02	0.5	100	32.2
C2		0.10			36.7
C3		0.50			42.8
C4		2.0			34.3

85 °C, 1 g/L (solid/liquid), 1000 rpm, k_{ss} values are based on slopes of linear relationships as in Fig. 4b (see text).

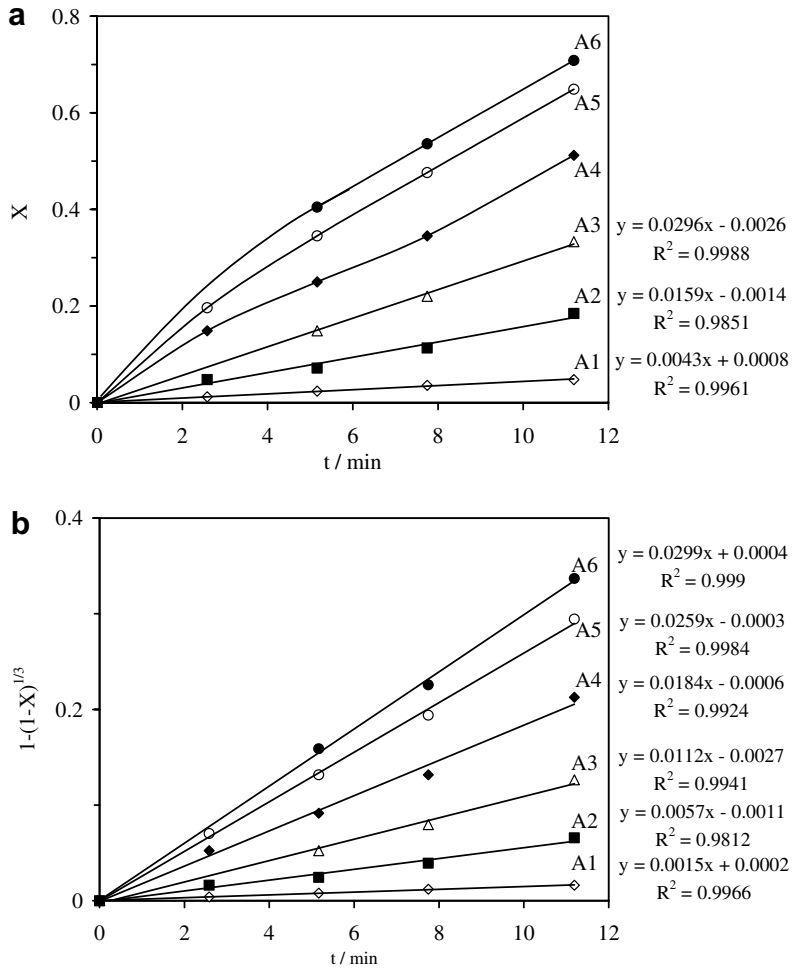

Fig. 4. Effect of oxygen concentration in the bubbling gas on: (a) fraction (X) of copper leached from chalcocite, (b) $1-(1-X)^{1/3}$ (A1–A6 described in Table 3).

reaction over 10–15 min. The linear relationships show the applicability of Eq. (1). Likewise, plots of $1-(1-X)^{1/3}$ versus t based on the results in sets B and C also gave good linear relationships and the relevant values of k_{ss} based on slopes are listed in Table 3.

Differentiation of Eq. (1) gives Eqs. (22) and (23). For low values of X, $(1-X)$ is close to 1 and therefore the ratio $(dX/dt)/k_{ss}$ should be close to 3 according to Eq. (23). The validity of this relationship is shown in Table 4 for tests A1–A3. The ratio $(dX/dt)/k_{ss}$ based on the linear correlations in Fig. 4a–b is close to 3, especially in set A1 (Table 4), which corresponds to low oxygen concentration and hence slow reaction. This is invalid at high oxygen concentrations (A4–A6 in Fig. 4a), due to the faster surface reaction and the larger values of X, leading to the inequality $(1-X) \neq 1$.

$$-(1/3)(1-X)^{-2/3}(-dX) = k_{ss}\,dt \tag{22}$$

$$dX/dt = 3k_{ss}(1-X)^{2/3} \tag{23}$$

Tromans (1998) reported Eq. (24) which shows the solubility dependence of oxygen concentration (C mol kg^{-1}) on temperature (T K) and pressure (P atm):

$$\ln\frac{C\,(\mathrm{mol/kg})}{P\,(\mathrm{atm})} = \frac{0.046T^2+203.35T\ln(T/298)-(299.378+0.092T)(T-298)-20591}{8.3144T} \tag{24}$$

This was used to calculate the concentration of dissolved oxygen at different oxygen pressures relevant to set A and the results are listed in Table 5. Fig. 5 compares the relative effects of increase in oxygen partial pressure and concentration of sodium chloride and sulphuric acid on dissolved oxygen at 85 °C (Tromans, 1998). The significant change in dissolved oxygen concentration shows the importance of considering the effect of both background reagent

Table 4
Comparison between dX/dt and k_{ss}

Test	O_2 content (%)	$10^5\,dX/dt$ (s^{-1})	$10^5 k_{ss}$ (s^{-1})	$\{dX/dt\}/k_{ss}$
A1	5	7.2	2.5	2.9
A2	21	26	9.5	2.7
A3	39	49	19	2.6

Based on Fig. 4a and b.

Table 5
The predicted effect of oxygen content of the bubbling gas on dissolved oxygen concentration in water

Test	O_2 content (%)	P_{O_2} (atm.)	$[O_2]$ (mol/t)
A1	5	0.05	0.039
A2	21	0.21	0.165
A3	39	0.39	0.307
A4	59	0.59	0.464
A5	81	0.81	0.637
A6	100	1.00	0.786

85 °C, based on Eq. (24) reported by Tromans (1998).

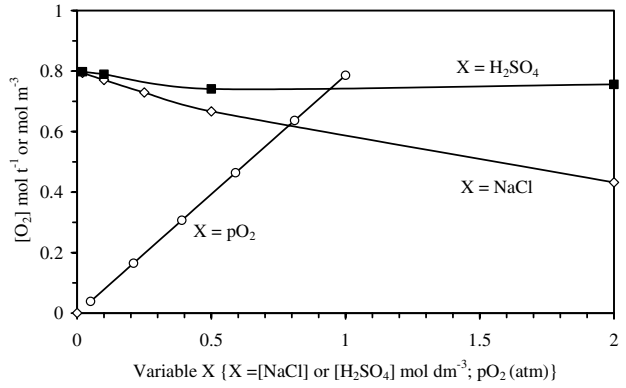

Fig. 5. Effect of oxygen partial pressure or concentration of background sodium chloride or sulphuric acid on oxygen solubility at 85 °C (data from Table 5 and Tromans (1998).

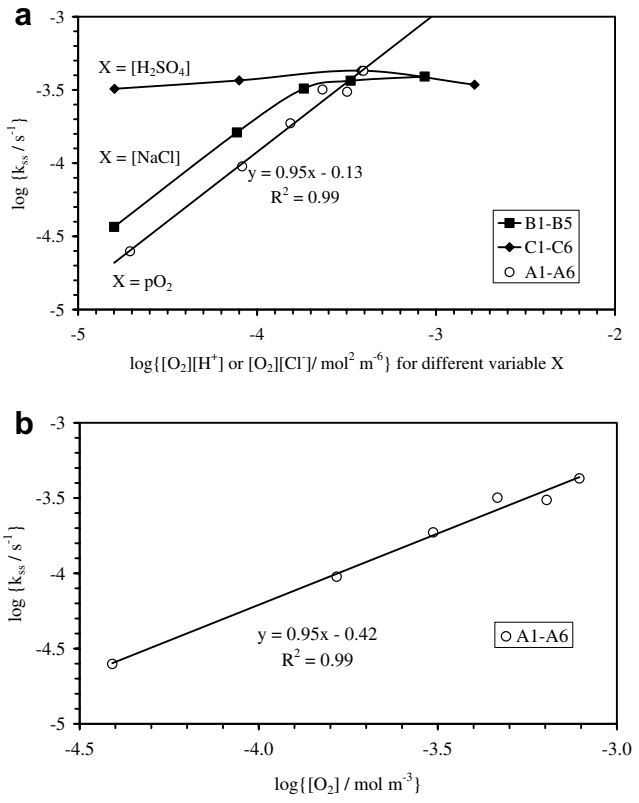

Fig. 6. Log–log plots k_{ss} versus $[O_2][Cl^-]$ or $[O_2][H^+]$ (a), or $[O_2]$ (b) in the three sets A1–A6, B1–B5 and C1–C4 (data from Table 3 and Fig. 5).

as well as the actual concentration of dissolved oxygen in rate analysis.

Fig. 6a shows a log–log plot of k_{ss} versus the concentration products $[O_2][H^+]$ or $[O_2][Cl^-]$. From the slopes it is clear that the surface reaction is zero order with respect to H^+ ions, while first order with respect to dissolved oxygen concentration. In the case of Cl^- ions the reaction order is unity at low concentrations, but it decreases to zero at higher concentrations ($\geqslant 0.5$ mol dm^{-3}).

5. Mass transfer coefficient

Cheng and Lawson (1991a) investigated the effect of stirring speed and particle size (12, 36 and 58 μm) on the rate of leaching in a mixture of sulphuric acid (0.5 mol dm^{-3}) and sodium chloride (0.5 mol dm^{-3}) at 85 °C. The rate of copper leaching from a sample of monosized particles was found to be independent of the stirring speed once the particles were fully suspended (at 1000 rpm), and the limiting thickness of the boundary layer was established around each particle. Based on the effect of particle size, Cheng and Lawson (1991a) concluded that the rate controlling step in the first leaching stage is diffusion of oxygen through the liquid boundary layer of the particles, due to the substantially low concentration of dissolved oxygen compared to other reagents.

This can be further investigated using Eqs. (25)–(28) (Cussler, 1997):

$$k_m = \frac{ShD}{L} \tag{25}$$

$$Sh = 2 + 0.6Gr^{1/4}Sc^{1/3} \tag{26}$$

$$Gr = \frac{L^3 g(\Delta\rho/\rho)}{v^2} \tag{27}$$

$$Sc = \frac{v}{D} \tag{28}$$

where Sh, Sherwood number; Gr, Grashof number; Sc, Schmidt number; D, diffusion coefficient; L, characteristic length (diameter); $\Delta\rho/\rho$, fractional density change; υ, kinematic viscosity.

For example, Raschman and Fedorockova (2006) investigated the rate of dissolution of magnesium oxide in hydrochloric acid solutions and calculated a value for the external mass transfer coefficient ($k_m = 6$–7×10^{-4} m s^{-1}) based on the diffusivity of HCl. They reported that the reaction rate constant for individual runs based on a shrinking sphere kinetic model (k in Eq. (1)) for the dissolution of magnesium oxide by HCl was three orders of magnitude lower than the external mass transfer coefficient. Miller and Wan (1983) also noted that the reaction velocity constant (1.3×10^{-5} m s^{-1}) for the first order dissolution of manganese dioxide by sulphurdioxide at different agitation speeds was an order of magnitude smaller than the expected mass transfer coefficient of sulphurdioxide to suspended particles (2.4×10^{-4} m s^{-1}). McCarthy et al. (1998) estimated a mass transfer coefficient of the

Table 6
Calculated mass transfer coefficients of oxygen to particles suspended in water

Particle	Size (μm)	$D(O_2)$ ($m^2\ s^{-1}$)[a]	υ ($m^2\ s^{-1}$)[b]	$\Delta\rho/\rho$	Gr	Sc	Sh	k_m ($m\ s^{-1}$)[c]
Au	10×10^{-3}	2×10^{-9}	9×10^{-7}	0.95	1.2×10^{-11}	450	2.00	0.4 (at 25 °C)
Cu_2S	23	6×10^{-9}	2.5×10^{-7}	0.82	1.6×10^{0}	42	4.30	1×10^{-3} (at 85 °C)

[a] Based on Stokes–Einstein equation (Cussler, 1997) at 25 and 85 °C.
[b] Haywood (1990).
[c] Eqs. (25)–(28).

order 0.1 m s^{-1} for the transfer of dissolved oxygen to gold colloids in diluted colloidal gold dispersions in aerated cyanide solutions. This value was in reasonable agreement with the value of 0.3 m s^{-1} predicted from a hydrodynamic treatment of the diffusion layer (McCarthy et al., 1998). However, in the case of gelatin stabilized gold colloids the rate constant for the surface reaction based on a shrinking sphere kinetic model (10^{-4} m s^{-1}) was three orders of magnitude smaller than the estimated mass transfer coefficient of oxygen.

Based on the values of D and υ, the calculated values of Gr, Sc, Sh, and k_m for the transport of oxygen to a gold particle and chalcocite particle are compared in Table 6 at 25 and 85 °C, respectively. The value of $k_m = 0.4$ m s^{-1} for colloidal gold of particle size 10 nm (assuming a density of 19.3 g cm^{-3}) is in reasonable agreement with the value in the range 0.1–0.3 m s^{-1} reported by McCarthy et al. (1998). In the case of chalcocite of density 5.65 g cm^{-3} (Kelly and Spottiswood, 1997) and particle size 23 μm, the calculated value of k_m is 1×10^{-3} m s^{-1}.

Following the procedure adopted by previous researchers (Miller and Wan, 1983; McCarthy et al., 1998; Raschman and Fedorockova, 2006) it is important to determine a value of k based on Eq. (1), so that it can be compared with k_m for Cu_2S listed in Table 6. Thus, Fig. 6b plots $\log k_{ss}$ as a function of $\log[O_2]$ for Set A1–A6 in Table 3, which gives an approximately linear relationship with an intercept given by Eq. (29).

$$\text{intercept} = \log\left(\frac{bk}{r_0\rho_{Cu}}\right) = -0.42 \tag{29}$$

Based on the density of chalcocite and a particle diameter 23 μm, the value of $r_0\rho_{Cu}$ is 0.82 mol m^{-2}. The substitution of this value along with $b = 2$ (Eq. (19)) gives $k = 0.2$ m s^{-1} at 85 °C. This value is two orders of magnitude larger than the value of $k_m = 1\times10^{-3}$ m s^{-1} (Table 6), indicating the influence of chloride ions on surface reaction. Cussler (1997) noted that in some heterogeneous reactions the diffusion of reactants coupled with a surface reaction could lead to faster reaction rates than expected from mass transfer calculations.

6. Reaction mechanism

The overall reaction shown in Eq. (19) can be described by a number of intermediate surface reaction steps to explain the reaction orders evident in Fig. 6a. Eqs. (30) and (31) show the adsorption of H_3O^+, Cl^-, and O_2 onto the solid surface leading to the rate controlling step shown by Eq. (32) which produces $Cu(OH)Cl^0$ as an interim copper species, covellite, and hydrogen peroxide. While $Cu(OH)Cl^0$ reacts with HSO_4^- according to Eq. (33), hydrogen peroxide disproportionates to H_2O and $0.5O_2$ according to Eq. (34). The overall reaction described in Eq. (35) is of the same form as Eq. (19) reported by Cheng and Lawson (1991a).

$$Cu_2S + H_3O^+ \rightarrow Cu_2S\cdot H_3O^+_{(ads)} \tag{30}$$

$$Cu_2S\cdot H_3O^+_{(ads)} + Cl^- + O_2 = Cu_2S\cdot H_3O^+\cdot Cl^-\cdot O_{2(ads)} \tag{31}$$

$$Cu_2S\cdot H_3O^+\cdot Cl^-\cdot O_{2(ads)} = CuS + Cu(OH)Cl^0_{(ads/aq)} + H_2O_2 \tag{32}$$

$$Cu(OH)Cl^0_{(ads/aq)} + HSO_4^- = Cu(SO_4)^0 + Cl^- + H_2O \tag{33}$$

$$H_2O_2 = H_2O + 0.5O_2 \tag{34}$$

$$Cu_2S + H_2SO_4 + 0.5O_2 = CuS + Cu(SO_4)^0 + H_2O \tag{35}$$

Hydrogen peroxide may also react with Cu_2S or CuS which would contain adsorbed $H_3O^+\cdot Cl^-$ according to Eqs. (36) and (37).

$$Cu_2S + H_3O^+\cdot Cl^- + H_2O_2 = CuS + Cu(OH)Cl^0 + 2H_2O \tag{36}$$

$$CuS + H_3O^+\cdot Cl^- + H_2O_2 = S + Cu(OH)Cl^0 + 2H_2O \tag{37}$$

The rates (dX/dt) based on anodic dissolution of chalcocite particles in a fluidised bed ($1–3\times10^{-5}$ s^{-1}, Table 7) are of the same order as the rate based on oxygen leaching using low oxygen partial pressure (7×10^{-5} s^{-1}, A1 in Table 4). Thus, the beneficial effect of chloride ions on the anodic dissolution of chalcocite in a fluidised bed (Eq. (21)) may also be related to the formation of $Cu(OH)Cl^0$ according to Eq. (38). The interim $Cu(OH)Cl^0$ species in Eqs. (36)–(38) will be converted to $Cu(SO_4)^0$ according to Eq. (33).

$$Cu_2S(s) + 0.9H_3O^+\cdot Cl^- = Cu_{1.1}S + 0.9Cu(OH)Cl^0 + 1.8H^+ + S + 1.8e^- \tag{38}$$

The simultaneous anodic (Eq. (16)) and cathodic (Eq. (18)) reactions on the chalcocite surface reported by previous researchers can now be written in the forms of Eqs. (39) and (40). These reactions incorporate the effect of chloride ions on the anodic reaction and the formation of peroxide

Table 7
Rates of fluid-bed anodic dissolution of synthetic Cu_2S in H_2SO_4–NaCl mixtures

Cu_2S (g)	NaCl (mol dm^{-3})[a]	Temperature (±1 °C)	Rate (stage 1) (g Cu/h)[a]	10^5 dX/dt (s^{-1})[b]
20	0	40	0.77[c]	1.3
10	0.43	40	0.60	3.3
20	0.85	40	0.70	1.2
20	0.85	90	0.77	1.3

[a] MacKinnon (1976), all systems contained H_2SO_4 1 mol dm^{-3}, anodic current 0.5 A, electrolyte flow rate 0.4 dm^3 min^{-1}.
[b] Based on 79.7% copper in synthetic chalcocite reported by MacKinnon (1976).
[c] At anode potential 0.68 V vs SCE.

in the cathodic reaction, while the sum gives the overall rate controlling reaction described by Eq. (32).

$$Cu_2S + H_3O^+ \cdot Cl^- = CuS + Cu(OH)Cl^0 + 2H^+ + S + 2e^- \quad (39)$$

$$Cu_2S + O_2 + 2H^+ + 2e^- = Cu_2S + H_2O_2 \quad (40)$$

At low pulp densities, in the presence of excess acid, the protonation of Cu_2S according to Eq. (30) would represent a rapid and complete adsorption reaction, while the overall reaction rate would depend on the fraction of protonated Cu_2S surface converted to $Cu_2S \cdot H_3O^+ \cdot Cl^- \cdot O_{2(ads)}$ denoted by θ. Equilibrium constant (K) for reversible adsorption reaction in Eq. (31), and the expression for θ are given by Eqs. (41) and (42).

$$K = \frac{\theta}{(1-\theta)[Cl^-][O_2]} \quad (41)$$

$$\theta = \frac{K[Cl^-][O_2]}{1 + K[Cl^-][O_2]} \quad (42)$$

Assuming that Eq. (32) is the rate controlling step, Eq. (43) gives the rate expression where R_{Cu} (mol m^{-2} s^{-1}) is the rate and k_{Cu} is the rate constant for the surface reaction; the latter represents the maximum rate per unit surface area at $\theta = 1$. The initial rates can also be calculated using Eq. (44) (Senanayake, 2007a). Thus, Eq. (43) can be written as Eq. (45) and the rearranged form in Eq. (46), which can be used to test the validity of this model to rationalise the effect of chloride and oxygen concentration on reaction rate.

$$R_{Cu} = k_{Cu}\theta = \frac{k_{Cu}K[Cl^-][O_2]}{1 + K[Cl^-][O_2]} \quad (43)$$

$$R_{Cu} = r_0\rho_{Cu}k_{ss} \quad (44)$$

$$\frac{1}{r_0\rho_{Cu}k_{ss}} = \frac{1}{k_{Cu}K[Cl^-][O_2]} + \frac{1}{k_{Cu}} \quad (45)$$

$$\frac{1}{k_{ss}} = \left(\frac{r_0\rho_{Cu}}{k_{Cu}K}\right)\frac{1}{[Cl^-][O_2]} + \left(\frac{r_0\rho_{Cu}}{k_{Cu}}\right) \quad (46)$$

Fig. 7 plots $(k_{ss})^{-1}$ as a function of $\{[Cl^-][O_2]\}^{-1}$. The two linear relationships in Fig. 7 support Eq. (46). The different slopes and intercepts for the data sets A1–A6, B1–B5, and B1–B3 listed in Table 8, based on Fig. 7, can be related to the different initial particle sizes 23×10^{-6} m and 31×10^{-6} m used in the batch leaching experiments (Table 3). The use of the relevant value of $r_0\rho_{Cu}$ gives $k_{Cu} = 1.7 \times 10^{-3}$ mol m^{-2} s^{-1} for set A1–A6. In the case of set B1–B3 where low chloride concentrations (<0.5 mol dm^{-3}) are considered, the value of $k_{Cu} = 1.5 \times 10^{-3}$ mol m^{-2} s^{-1} is in good agreement with the value calculated for set A1–A6.

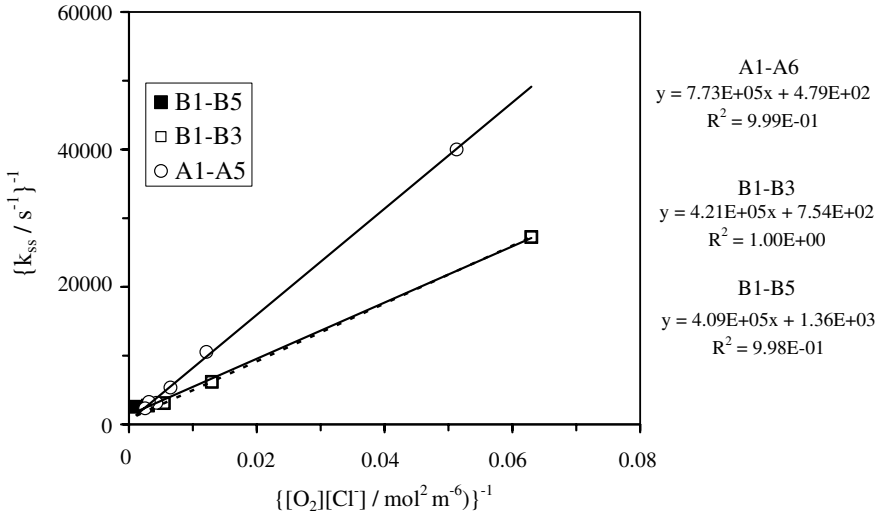

Fig. 7. Linear variation of $(k_{ss})^{-1}$ as a function of $[O_2][Cl^-]^{-1}$ for sets A1–A6 and B1–B3, or B1–B5 in Table 2 (data from Table 3 and Fig. 5).

Table 8
The slopes, intercepts and k_{Cu} based on Fig. 7

Set	Slope	Intercept	r_0 (m)	$r_0\rho$ (mol m^{-2})	k_{Cu} (mol m^{-2} s^{-1})[a]
A1–A6	7.7×10^{5}	4.8×10^{2}	11.5×10^{-6}	0.82	1.7×10^{-3}
B1–B3	4.2×10^{5}	7.5×10^{2}	15.5×10^{-6}	1.10	1.5×10^{-3}
B1–B5	4.1×10^{5}	1.4×10^{3}	15.5×10^{-6}	1.10	0.8×10^{-3}

[a] Based on Eq. (46).

7. Summary and conclusions

The beneficial effect of low concentration of chloride ions on the leaching of base metal sulphides has been known since the late 1970s. The role of chloride as a complexing agent for cuprous ions has been ruled out by previous researchers. In the case of pressure oxidation by oxygen, the role of chloride has been treated as similar to the surfactants that disperse the molten sulphur and thus remove passivation of mineral surface by elemental sulphur. The observations during atmospheric oxidation of a chalcopyrite concentrate by oxygenated iron(III) sulphate at 95 °C and the analysis of rate data have supported the previous researchers to conclude the involvement of chloride ions in the surface reaction. The present study focussed on analysing the leaching kinetics of synthetic chalcocite by oxygenated sulphuric acid in the presence of sodium chloride at 85 °C, a temperature below the melting point of sulphur (113 °C).

The leaching results in the initial 10–15 min follow a shrinking sphere kinetic model indicating that the rate is controlled by a surface reaction, with apparent rate constants indicating a first order reaction with respect to dissolved oxygen concentration, but zero order with respect to hydrogen ion concentration. The first order dependence of the apparent rate constant on chloride ion concentration in the range 0.02–0.25 mol dm^{-3} shows the involvement of chloride ions in the surface reaction. The rate constant for the conversion of Cu_2S to CuS and Cu(II) by oxygenated sulphuric acid in the presence of chloride, based on a shrinking particle (sphere) model (0.2 m s^{-1}), is two orders of magnitude larger than the calculated mass transfer coefficient based on oxygen transfer (1×10^{-3} m s^{-1}). This also indicates the involvement of chloride ions in the surface reaction.

The proposed surface reaction involves the following steps: (i) rapid adsorption of H_3O^+ onto Cu_2S to produce $Cu_2S(H_3O^+)$ and equilibration with Cl^- and O_2 to produce $Cu_2S(H_3O^+)(Cl^-)(O_2)$; (ii) rate controlling reaction to produce CuS, $Cu(OH)Cl^0$ and H_2O_2; (iii) reaction of $Cu(OH)Cl^0$ with HSO_4^- to produce $Cu(SO_4)^0$ and Cl^-; and (iv) decomposition of H_2O_2 to H_2O and $0.5O_2$ or reaction of H_2O_2 with Cu_2S or CuS. The rate constant for the surface reaction converting Cu_2S to CuS and Cu(II) is of the order 10^{-3} mol m^{-2} s^{-1}.

References

Berezowsky, R., Trytten, L., 2002. Commercialization of the acid pressure leaching of chalcopyrite. ALTA Copper. Perth, Australia.

Brown, J.A., Papangelakis, G., 2005. Interfacial studies of liquid sulphur during aqueous pressure oxidation of nickel sulphide. Miner. Eng. 18, 1378–1385.

Carneiro, M.F.C., Leao, V.A., in press. The role of sodium chloride on surface of chalcopyrite leached with ferric sulfate. Hydrometallurgy.

Cheng, Y.C., Lawson, F., 1991a. The kinetics of leaching chalcocite in acidic oxygenated sulphate–chloride solutions. Hydrometallurgy 27, 249–268.

Cheng, Y.C., Lawson, F., 1991b. The kinetics of leaching covellite in acidic oxygenated sulphate–chloride solutions. Hydrometallurgy 27, 269–284.

Claassen, J.O., Meyer, E.H.O., Rennie, J., Sandenbergh, R.F., 2003. Iron precipitation from zinc-rich solutions: optimizing the Zincor process. J. South Afr. Inst. Min. Metall. 103, 253–263.

Cussler, E.L., 1997. Diffusion: Mass Transfer in Fluid Systems. Cambridge University Press.

Deng, T., Lu, Y., Wen, Z., Liu, D., 2001. Oxygenated chloride-assisted leaching of copper residue. Hydrometallurgy 62, 23–30.

Defreyne, J., Grieve, W., Jones, D.L., Mayhew, K., 2006. The role of iron in CESL process. In: Dutrizac, J.E., Riveros, P.A. (Eds.), Iron Control Technologies (Proc. 3rd International Symposium). Canadian Institute of Mining, Metallurgy, and Petroleum, Montreal, pp. 205–220.

Dreisinger, D., 2006. Copper leaching from primary sulfides: options for biological and chemical extraction of copper. Hydrometallurgy 83, 10–20.

Dreisinger, D.B., Steyl, J.D.T., Sole, K.C., Gnoinski, J., Dempsey, P., 2003. The Anglo American Corporation/University of British Columbia (AAC/UBC) chalcopyrite process: an integrated pilot plant evaluation. In: Riveros, P.A., Dixon, D., Dreisinger, D.B., Menacho, J. (Eds.), Hydrometallurgy of Copper 1: Leaching and Process Development. Canadian Institute of Mining, Metallurgy, and Petroleum, Montreal, pp. 223–238.

Dixon, D.G., Petersen, J., 2003. Comprehensive modelling study of chalcocite column and heap bioleaching. In: Riveros, P.A., Dixon, D., Dreisinger, D.B., Menacho, J. (Eds.), Hydrometallurgy of Copper: Modelling, Impurity Control, and Solvent Extraction. Canadian Institute of Mining, Metallurgy, and Petroleum, Montreal, pp. 493–516.

Ferron, C.J., Fleming, C.A., O'Kane, P.T., Dreisinger, D., 2002. High temperature chloride assisted leach process to extract simultaneously Cu, Ni, Au and PGM's from various feedstocks. In: Peek, E., Van Weert, G. (Eds.), Chloride Metallurgy. CIM, Montreal, pp. 11–28.

Ferron, C.J., Fleming, C.A., Dreisinger, D., O'Kane, T.O., 2003. Chloride as an alternative to cyanide for the extraction of gold – going full circle? In: Hydrometallurgy 2003 – Fifth International Conference in Honor of Professor Ian Ritchie, Vol. 1. TMS, Warrendale, pp. 89–104.

Flynn, C.M., 1984. Hydrolysis of inorganic iron(III) salts. Chem. Rev. 84, 31–41.

Grewal, I., Dreisinger, D.B., Krueger, D., Tyroler, P.M., Krause, E., Nissen, N.C., 1992. Total oxidative leaching of Cu_2S-containing residue at INCO Ltd.'s copper refinery: laboratory studies on the reaction pathways. Hydrometallurgy 29, 319–333.

Haywood, R.W., 1990. Thermodynamic Tables in SI Units. Cambridge University Press, UK.

Hine, F., Yamakawa, K., 1970. Mechanism of oxidation of cuprous ion in hydrochloric acid solution by oxygen. Electrochim. Acta 15, 769–781.

Hogfeldt, E., 1982. Stability Constants of Metal-Ion Complexes, 2nd Supplement, IUPAC Chemical Data Series No. 2, Part A, Inorganic Ligands. Pergamon, Oxford.

Johnson, G.D., Streltsova, N., 1999. Method for the processing of copper minerals. US Patent 3,856,913, December 24, 1974.

Kelly, E.G., Spottiswood, D.J., 1997. Introduction to Mineral Processing. Australian Mineral Foundation.

Levenspiel, O., 1972. Chemical Reactions Engineering. Wiley, New York.

Lu, Z.Y., Jeffrey, M.I., Zhu, Y., Lawson, F., 2000a. Studies of pentlandite leaching in mixed oxygenated acidic chloride–sulphate solutions. Hydrometallurgy 56, 63–74.

Lu, Z.Y., Jeffrey, M.I., Lawson, F., 2000b. The effect of chloride ions on the dissolution of chalcopyrite in acidic solutions. Hydrometallurgy 56, 189–202.

Mao, M.H., Peters, E., 1983. Acid pressure leaching of chalcocite. In: Osseo-Asare, K., Miller, J.D. (Eds.), Hydrometallurgy: Research, Development and Plant Practice. Metall. Soc. AIME, Warrendale, PA, pp. 243–260.

MacKinnon, D.J., 1976. Fluidised-bed anodic dissolution of chalcocite. Hydrometallurgy 1, 241–257.

McCarthy, A.J., Coleman, R.G., Nicol, M.J., 1998. The mechanism of the oxidative dissolution of colloidal gold in cyanide media. J. Electrochem. Soc. 145, 408–414.

McDonald, G.W., Saud, A., Barger, M.S., Koutsky, J.A., Langer, S.H., 1987. The fate of gold in cupric chloride hydrometallurgy. Hydrometallurgy 18, 321–336.

McDonald, R.G., Muir, D.M., 2007. Pressure oxidation leaching of chalcopyrite Part II: Comparison of medium temperature kinetics and products and effect of chloride ion. Hydrometallurgy 86, 206–220.

McDonald, G.W., Langer, S.H., 1983. Cupric chloride leaching of model sulfur compounds for simple copper ore concentrates. Metall. Trans. 14B, 559–570.

Mendez De Leo, L.P., Bianchi, H.L., Fernandez-Prini, R., 2005. Ion pair formation in copper sulphate aqueous solutions at high temperatures. J. Chem. Thermodyn. 37, 499–511.

Miki, H., Hiroyoshi, N., Kuroiwa, S., Tsunekawa, M., Hirajima, T., 2003. Mechanisms of catalytic leaching of chalcopyrite. In: Riveros, P.A., Dixon, D., Dreisnger, D.B., Menacho, J. (Eds.), Hydrometallurgy of Copper 1: Leaching and Process Development. Canadian Institute of Mining, Metallurgy, and Petroleum, Montreal, pp. 383–394.

Miller, J.D., Wan, R.Y., 1983. Reaction kinetics for the leaching of MnO_2 by sulfur dioxide. Hydrometallurgy 10, 219–242.

Muir, D.M., 2002. Basic principles of chloride hydrometallurgy. In: Peek, E., Van Weert, G. (Eds.), Chloride Metallurgy 2002. CIM, Montreal, pp. 255–276.

Muir, D.M., Ho, E., 1996. Composition and electrochemistry of nickel matte: Implication for matte leaching and refining in acid solutions. In: Grimsey, E.J., Neuss, I. (Eds.), Nickel'96. AusIMM, Victoria, pp. 291–297.

Nicol, M.J., Lazaro, I., 2003. The role of non-oxidative processes in the leaching of chalcopyrite. In: Riveros, P.A., Dixon, D., Dreisnger, D.B., Menacho, J. (Eds.), Hydrometallurgy of Copper 1: Leaching and Process Development. Canadian Institute of Mining, Metallurgy, and Petroleum, Montreal, pp. 367–381.

Okamoto, H., Nakayama, R., Tsunekawa, M., Hiroyoshi, N., 2003. Improvement of chalcopyrite leaching in acidic sulphate solutions by redox potential control. In: Riveros, P.A., Dixon, D., Dreisnger, D.B., Menacho, J. (Eds.), Hydrometallurgy of Copper: Leaching and Process Development. Canadian Institute of Mining, Metallurgy, and Petroleum, Montreal, pp. 67–81.

Parker, A.J., Paul, R.L., Power, G.P., 1981. Electrochemical aspects of leaching copper from chalcopyrite in ferric and cupric salt solutions. Aust. J. Chem. 34, 13–34.

Peters, E., 1976. Direct leaching of sulphides: chemistry and applications. Metall. Trans. 7B, 505–517.

Peacey, J., Guo, X.J., Robles, E., 2003. Copper hydrometallurgy – Currnet status, preliminary economics, future directions, and positioning versus smelting. In: Riveros, P.A., Dixon, D., Dreisnger, D.B., Menacho, J. (Eds.), Hydrometallurgy of Copper 1: Leaching and Process Development. Canadian Institute of Mining, Metallurgy, and Petroleum, Montreal, pp. 205–222.

Provis, J.L., van Deventer, J.S.J., Rademan, J.A.M., Lorenzen, L., 2003. A kinetic model for the acid-oxygen pressure leaching of Ni–Cu matte. Hydrometallurgy 70, 83–99.

Rademan, J.A.M., Lorenzen, L., van Deventer, J.S.J., 1999. The leaching characteristics of Ni–Cu matte in the acid-oxygen pressure leach process at Impala Platinum. Hydrometallurgy 52, 231–252.

Raschman, P., Fedorockova, A., 2006. Dissolution of periclase in excess of hydrochloric acid: Study of inhibiting effect of acid concentration on the dissolution rate. Chem. Eng. J. 117, 205–211.

Ruiz, M.C., Honores, S., Padilla, R., 1998. Leaching kinetics of digenite concentrate in oxygenated chloride media at ambient pressure. Metall. Mater. Trans. 29B, 961–969.

Ruiz, M.C., Abarzua, E., Padilla, R., 2007. Oxygen pressure leaching of white metal. Hydrometallurgy 86, 131–139.

Senanayake, G., 2007a. Review of rate constants for thiosulphate leaching of gold from ores, concentrates, and flat surfaces: effect of host minerals and pH. Miner. Eng. 20, 1–15.

Senanayake, G., 2007b. Review of theory and practice of measuring proton activity and pH in concentrated chloride solutions and application to oxide leaching. Miner. Eng. 7, 634–645.

Senanayake, G., Muir, D.M., 1988. Speciation and Reduction potentials of metal ions in concentrated chloride and sulphate solutions relevant to processing base metal sulfides. Metall. Trans. 19B, 37–45.

Senanayake, G., Muir, D.M., 2003. Chloride processing of metal sulphides: review of fundamentals and applications. In: Hydrometallurgy 2003 – Fifth International Conference in Honor of Professor Ian Ritchie, Vol. 1. TMS, Warrendale, pp. 517–531.

Sillen, L.G., Martell, A.E., 1964. Stability constants of metal complexes. In: Chemical Society Special Publication, vols. 17 and 26. Chemical Society, London.

Subramanian, K.N., Ferrajuolo, R., 1976. Oxygen pressure leaching of Fe–Ni–Cu sulfide concentrates at 110 °C – effect of chloride addition. Hydrometallurgy 2, 117–125.

Sullivan, J.D., 1933. Chemical and physical features of copper leaching. Trans. Am. Inst. Min. Metall. 106, 515–547.

Taylor, A., 1995. Copper leach/SX/EW Project Development. Alta Metallurgical Services, Brisbane.

Tromans, D., 1998. Temperature and pressure dependent solubility of oxygen in water: a thermodynamic analysis. Hydrometallurgy 48, 327–342.

Tshilombo, A.F., Dixon, D.G., 2003. Mechanism of chalcopyrite passivation during bacterial leaching. In: Riveros, P.A., Dixon, D., Dreisnger, D.B., Menacho, J. (Eds.), Hydrometallurgy of Copper 1: Leaching and Process Development. Canadian Institute of Mining, Metallurgy, and Petroleum, Montreal, pp. 99–116.

Vracar, R.Z., Parezanovic, I.S., Cerovic, K.P., 2000. Leaching of copper(I) sulfide in calcium chloride solution. Hydrometallurgy 58, 261–267.